JOURNAL OF Materials CHEMISTRY

An X-ray absorption study on copper-containing $AlPO_4$-5 for selective catalytic reduction of NO_X by propene

Ian D. Burton,[a] Justin S. J. Hargreaves,[a] David G. Nicholson,*[b] Merete H. Nilsen[b] and Michael Stockenhuber[a]

[a]*The Catalysis Research Laboratory, Department of Chemistry and Physics, The Nottingham Trent University, Clifton Campus, Clifton Lane, Nottingham, UK NG11 8NS*
[b]*Department of Chemistry, Norwegian University of Science and Technology, N-7491 Trondheim, Norway. E-mail: david.nicholson@chembio.ntnu.no*

Received 9th November 2000, Accepted 7th February 2001
First published as an Advance Article on the web 12th March 2001

A copper-containing $AlPO_4$-5 was synthesised using copper(II) acetate as the copper source. The local environments about copper in the as-synthesised and calcined materials have been studied using XANES and EXAFS. The results show that in the former copper is contained in $Cu(O)_4$ groupings which are linked to another $Cu(O)_4$ group at a Cu···Cu distance of 2.93 Å. On calcination the pairs separate with copper increasing its coordination to give a distorted $Cu(O)_6$ entity which is not incorporated into the $AlPO_4$-5 framework but linked to it *via* an $(OAl/P–)_2$ connectivity. This shows that copper(II) acetate is not a source for framework substitution of copper. For comparison Cu : $AlPO_4$-5 was prepared in which copper was incorporated by the incipient wetness method. The EXAFS of the latter shows that copper is present in several environments, probably interacting with framework oxygen atoms.

The activities of these materials towards the selective catalytic reduction of NO_X to N_2 in the presence of hydrocarbons and oxygen was measured. CuAPO-5/$CuAc_2$ and Cu : $AlPO_4$-5 both show low activity for this reaction (16.8% at 400 °C and 11.8% at 500 °C, respectively). The XANES show that autoreduction does not occur for these materials. This contrasts with CuZSM-5 which is an efficient catalyst for the same reaction and undergoes autoreduction.

Introduction

Since the discovery of the microporous aluminophosphates in 1982,[1] a number of metals are known to substitute for the framework atoms aluminium or phosphorus (ref. 2 and references cited therein). Divalent metals that substitute Al(III) are particularly interesting because they create Brønsted acid sites thereby improving catalytic properties.[3] Attempts to incorporate copper(II) into zeotype frameworks failed[4–6] until a material (CuAPO-5) was obtained from the hydrothermal synthesis of $AlPO_4$-5 in the presence of copper oxide as the source of copper; EPR, ESEM[7] and XAS (XANES and EXAFS)[2] together show that copper is actually sited in the $AlPO_4$-5 framework.

Several copper-containing zeotypes have been found to catalyse the decomposition of NO_X.[8] One of them, the copper ion-exchanged zeolite Cu-ZSM-5, has been extensively studied, particularly in the selective catalytic reduction of NO_X in the presence of hydrocarbons and oxygen.[9–12]

There is also interest in studying zeotypes that incorporate copper(II) in ways other than by ion-exchange. Examples include the microporous aluminophosphates. Catalytic activity has been reported for CuAPO-5 (see above) in the selective catalytic reduction of NO_X in the presence of ammonia and oxygen.[2] This material, prepared from copper(II) oxide, exhibits lower activity than that prepared using copper(II) acetate as the copper source. This difference in chemical properties apparently stems from their different modes of incorporating copper. These observations are significant because they accord with the structural differences. It is known that copper(II) acetate does not function as a source of copper in the same manner as copper(II) oxide.[7] The reason for this has not been clearly established but it may possibly be related to the chelating properties of the acetate ligand restricting the incorporation of copper(II) into the framework.

X-Ray absorption spectroscopy (XAS) is a widely used method for characterising local structural features of selected elements in heterogeneous catalysts. In particular, although the technique is actually a bulk technique it is also valuable for studying chemical reactions that take place at the surfaces of heterogeneous catalysts because the overall contribution to the XAS signal arises from the significant proportion of active sites that are highly dispersed over a large number of surfaces. XAS has been used extensively to study local metal environments in a number of zeotypes. Examples include metal-substituted microporous alumino- and silicoalumino-phosphates (AlPO's and SAPO's)[13–15] and the cations in ion-exchanged zeolites, *e.g.* the copper-containing zeolite deNO_X catalysts.[12,16,17]

We report here the results of XRD, XAS and deNO_X measurements (in the presence of hydrocarbons and oxygen) for CuAPO-5 derived from copper(II) acetate (CuAPO-5/$CuAc_2$). These results are compared with those for non-framework copper in Cu : $AlPO_4$-5 (in which copper was introduced by the incipient wetness method) and for the previous reported framework substituted copper in CuAPO-5 derived from copper(II) oxide (CuAPO-5/CuO). It is shown that substitution of copper into the framework does not occur with copper(II) acetate under these conditions, and that the materials exhibit low catalytic activity towards NO_X in the presence of propene.

Experimental

Synthesis

CuAPO-5/$CuAc_2$ was prepared according to a similar routine as previously reported.[2] The copper source, copper acetate

DOI: 10.1039/b009024g

(2.0 g), orthophosphoric acid (6.8 ml; H_3PO_4, 85 wt%, Merck) and deionised water (18.2 ml) were mixed and stirred until a blue solution was obtained (30 minutes). To this solution was added pseudo-boehmite (7.3 g; AlOOH, BA Chemicals Ltd.), and the mixture stirred until a homogenous gel appeared (1.5 hour), at this stage the template, tetraethylammonium hydroxide (18 ml; TEAOH, 40%, Aldrich) was added, and the gel stirred for another hour. The resulting turquoise-coloured gel (pH 3) was transferred into Teflon-lined stainless-steel bombs, and heated at 150 °C for 24 hours.

Crystallisation was accompanied by an increase in pH to 7. The crystalline, turquoise-coloured product was filtered, washed with deionised water and dried in air at room temperature. The material was calcined in air at 550 °C for 24 hours. The colour of the calcined products was light green.

For the incipient wetness procedure, pure $AlPO_4$-5 was synthesised according to the method reported by Tapp *et al.*[18] To the sample (1.2 g) was added $Cu(NO_3)_2$ (1.0 M, 1.0 ml). The turquoise material was washed with distilled water, filtered, and dried at 100 °C. The colour changed to light green upon calcination in air at 550 °C for 24 hours.

Characterisation

The identity of the samples was checked by X-ray powder diffraction using a Siemens D-5005 diffractometer, equipped with a scintillation detector and Cu Kα radiation (Cu Kβ was removed by a Ni filter). The copper content was determined by atomic absorption spectroscopy (AAS) on a Perkin Elmer 1100 B AAS using the flame technique. The copper contents for CuAPO-5 and Cu : AlPO4-5 are 5.0 and 5.7 wt%, respectively.

X-Ray absorption data collection

XAS data were collected using the European Synchrotron Radiation Facility (ESRF) (energy 6.0 GeV, max. current 200 mA). Spectra were obtained from the Swiss-Norwegian beamline (SNBL), at the copper K-edge ($\lambda = 1.38043$ Å, $E = 8979$ eV).

The monochromator was a channel cut Si(111) single crystal. Higher-order harmonics (*ca.* two orders of magnitude) were rejected by means of a gold-coated mirror angled at 7.3 mrad from a beam of size 0.6 × 4.7 mm which was defined by the slits in the station. The maximum resolution ($\Delta E/E$) of the Si(111) bandpass is 1.4×10^{-4}.

Gas ion chambers were used for measuring the intensities of the incident (I_0) and transmitted (I_t) X-rays. The detector gases were as follows: I_0, detector length 17 cm, 97.1% N_2, 2.9% Ar; I_t, length 31 cm, 49.5% N_2, 50.5% Ar.

The amounts of material in the samples were calculated from element mass fractions and the absorption coefficients of the constituent elements[19] above the absorption edge to give an absorber optical thickness of 1.5 absorption lengths. The well-powdered (50–100 mg) samples were mixed with boron nitride so as to obtain a homogeneous sample thickness of *ca.* 1 mm for a surface area of 1.2 cm^2 and placed in aluminium sample holders and held in place by Kapton tape. Data were collected over the energy range 8867–9988 eV. Several scans were collected and summed.

EXAFS data analysis

The data were corrected for dark currents, summed, deglitched and background subtracted to yield the EXAFS function $\chi_i^{obs}(k)$ by means of the EXCALIB and EXBACK programs.[20] The edge positions were determined from the first inflection points of the derivative spectra. Model fitting was carried out by EXCURV90,[20] using curved-wave theory and *ab initio* phase shifts calculated within EXCURV90. The low energy cut-off for all samples was 30 eV, and the k^3 weighting scheme was used.

The model compounds Tutton salt ($Cu(NH_4)_2(SO_4)_2 \cdot 6H_2O$),[21] copper(II) hydroxide[22] and copper(II) oxide[23] were used[2] to check the validity of the *ab initio* phase shifts and to establish the general parameters, AFAC and VPI.[24] These parameters were transferred to the analyses on the unknowns, thereby reducing any residual systematic error in the multiplicities.

The EXAFS spectra were least squares fitted using k^1 and k^3 weighted data. Coupling between N (multiplicity) and $2\sigma^2$ (Debye–Waller-type factor) was minimised by choosing solutions common to both weighting schemes.[25]

The k^3 weighting scheme used in the refinement compensates for the diminishing photoelectron wave at higher k. All of the spectra were treated in exactly the same manner and the validity of the data reduction and fitting procedures was checked against the spectra of the reference compounds. The data were analysed over the range $k = 3$–12 Å^{-1}, and the refinement carried out to minimise the fit index (FI):

$$\mathrm{FI} = \sum_i \left[k^3(\chi_i^{\exp} - \chi_i^{\mathrm{calc}})\right]^2$$

where $\chi_i^{\exp}$ and χ_i^{calc} are the experimental and theoretical EXAFS respectively.[20]

If meaningful results are to be obtained, it is essential to identify the maximum number of independent parameters, N_{ind}, that may be varied in the EXAFS analysis. This is given by $N_{\mathrm{ind}} = (2\Delta k \Delta R/\pi) + 2$ where Δk is the extent of the data in k-space and ΔR the range of distance being modelled.[26] For CuAPO-5 the maximum value corresponds to $N_{\mathrm{ind}} = 13$ ($\Delta R = 1.20$ Å) and for as-synthesised ($\Delta R = 1.35$ Å) and calcined ($\Delta R = 0.84$ Å) Cu : APO-5, $N_{\mathrm{ind}} = 14$ and 8, respectively. Another constraint is the smallest separation of shells that can be resolved. This is given by $\pi/\Delta k = 0.26$ Å.[27] The addition of successive shells was tested for significance using the procedure of Joyner *et al.*[28]

deNO$_X$ measurements

Catalytic experiments were carried out on a fixed bed microreactor.[16] The products were analysed by a chemiluminescent NO_X analyser (Signal Instruments Model 4000) and a gas chromatograph fitted with a thermal conductivity detector (Pye Unicam PU4550). The reaction mixture was analysed for propane, NO_X and CO_2. The catalysts were activated at 500 °C for one hour under a stream of 2% O_2/He. NO and hydrocarbon conversion was measured over the temperature range 500 °C–300 °C, using a reactant mixture of NO (2000 ppm), propene (1220 ppm) and 2% O_2, balanced with helium, over a bed volume of 1 ml (which corresponds to *ca.* 0.25 g) at a total reactant flowrate of 300 ml min^{-1}. The powdered catalysts were pelleted to 0.6–1 mm mesh size.

Results and discussion

Characterisation

Although the diffractogram for CuAPO-5/$CuAc_2$ confirms that the sample has the $AlPO_4$-5 (AFI) structure[29] and shows that the material is thermally stable at 550 °C, the splittings of some of the peaks in the latter are also consistent with the calcination inducing some changes in structural features.[30] In contrast, the diffractograms for Cu : APO_4-5 show that the $AlPO_4$-5 structure is little affected by the incorporation of copper.

XANES

Calcination of some copper(II) zeolites (*i.e.* Cu-ZSM-5[12] and Cu-β zeolite[2]) leads to autoreduction of copper(II) to copper(I). When studying the catalytic properties (see below) it is clearly important to establish if this behaviour also extends to the present two types of copper-containing zeotype.

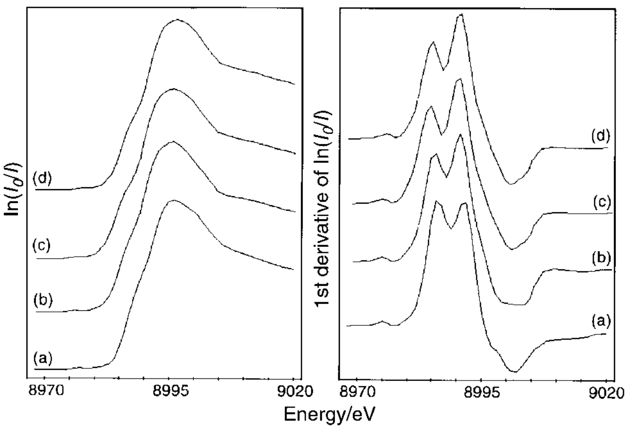

Fig. 1 Normalised Cu K-edge XANES and the first derivatives of (a) as-synthesised CuAPO-5/CuAc$_2$; (b) calcined CuAPO-5/CuAc$_2$; (c) as-synthesised Cu : AlPO$_4$-5; (d) calcined Cu : AlPO$_4$-5.

XANES spectra are convenient indicators of autoreduction because copper(I) spectra contain a characteristic intense pre-edge feature a few electronvolts below the edge (at *ca.* 8983–8986 eV).[31,32] It is clear from the XANES (particularly the first derivative spectra) of the present materials (Fig. 1) that autoreduction does not occur. This conclusion is supported by the very weak transition at 8979 eV (the formally dipole-forbidden 1s→3d transition) that is characteristic of copper(II) compounds.[31] The low intensity of this transition is consistent with a tetragonal rather than tetrahedral environment.[2]

In the XANES of copper(II) oxide there is a transition manifested by a shoulder or peaks about halfway up the absorption edge (8991 eV; 1s→4p transition).[33–35] Since this feature is not observed in the XANES of CuAPO-5/CuAc$_2$ (Fig. 1) copper(II) oxide is absent in this sample.

Similarly, the XANES of Cu : AlPO$_4$-5 (Fig. 1) show that autoreduction does not occur. Compared to the zeolites Cu-β2 and Cu-ZSM-5 which do exhibit autoreduction,[12] this result indicates that the non-framework siting of copper in the materials studied here differs significantly from the copper environments in the ion-exchanged zeolites. Moreover, XAS shows that Cu : AlPO$_4$-5 is unchanged on calcination.

EXAFS

The k^3-weighted experimental and least-squares fitted EXAFS spectra of CuAPO-5/CuAc$_2$ and Cu : AlPO$_4$-5 are shown in Fig. 2 and 3, respectively. Also shown in the figures are the corresponding Fourier transforms. Table 1 gives the results of the least-squares analyses.

CuAPO-5/CuAc$_2$

Because of the reluctance of copper to coordinate tetrahedrally, the multiplicity of four for the Cu–O distance at 1.93 Å more likely indicates a square planar rather than a tetrahedral environment. The shell at *ca.* 3.1 Å in the Fourier transformed EXAFS is a convenient indicator for framework substitution,[2] since substituting a metal (M) into a T (aluminium or phosphorus) site of the zeotype lattice leads to four M···T interactions at this distance.

For the as-synthesised CuAPO-5/CuAc$_2$, this shell is a composite peak in which copper is the major contributor showing that copper is distributed pairwise. Similar Cu···Cu interactions (2.93 Å) are found in copper oxide and impregnated Cu-ZSM-5.[16] The formation of clusters during the hydrothermal processes may be due to the chelating properties of the acetate anion, although the Cu···Cu distance in copper(II) acetate (2.64 Å[36]) is shorter than that in CuAPO-5/CuAc$_2$ (2.93 Å). On calcining CuAPO-5/CuAc$_2$, the clusters break down as the copper atoms distribute through the channels of the structure and interact with the framework through bridging oxygens (2 × Cu–O–Al) (aluminium was used to represent both T-atoms because the atomic numbers for these are too close to be unequivocally distinguished by EXAFS).

The multiplicities of the first shell (Cu–O) in the as-synthesised and calcined CuAPO-5/CuAc$_2$ materials are 4.0 and 6.0, respectively. In the as-synthesised sample, copper is

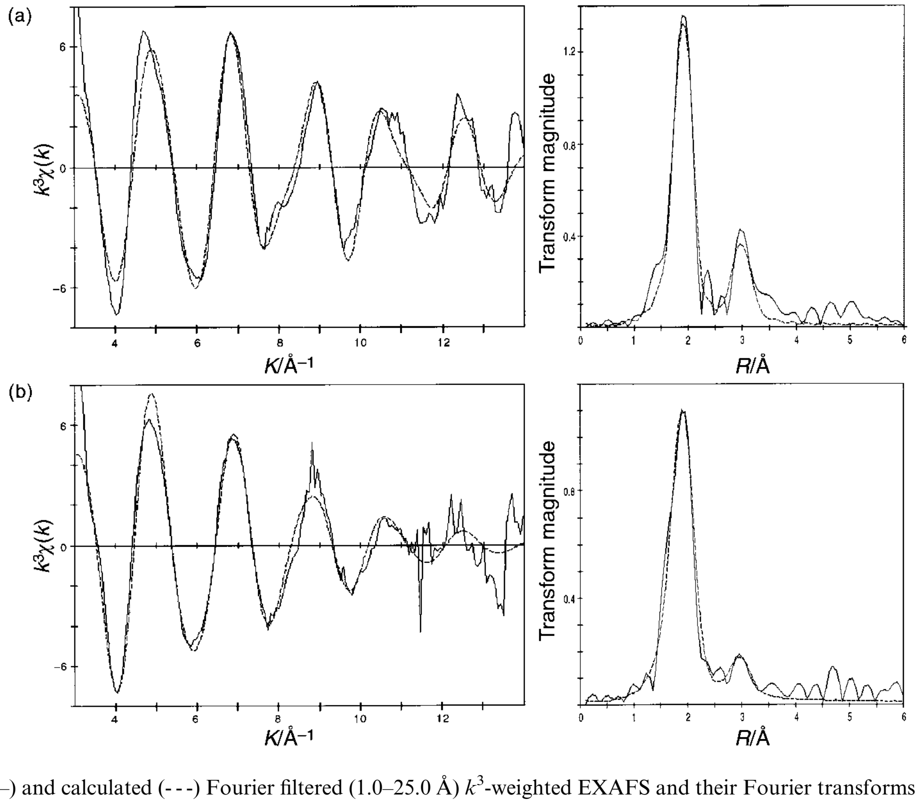

Fig. 2 Experimental (—) and calculated (- - -) Fourier filtered (1.0–25.0 Å) k^3-weighted EXAFS and their Fourier transforms for CuAPO-5/CuAc$_2$: (a) as-synthesised sample; (b) calcined sample.

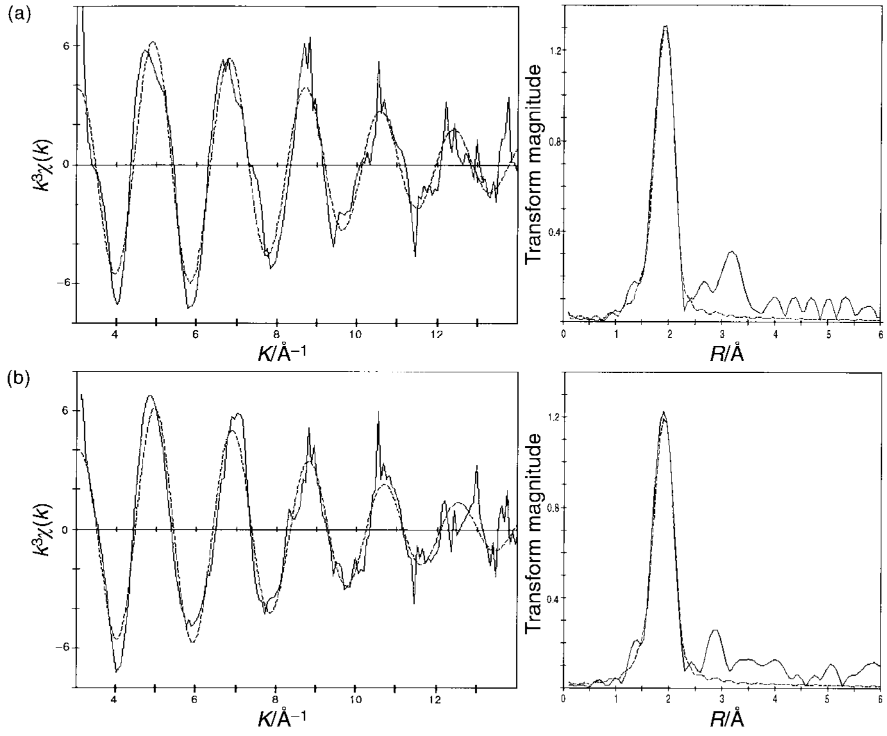

Fig. 3 Experimental (—) and calculated (- - -) Fourier filtered (1.0–25.0 Å) k^3-weighted EXAFS and their Fourier transforms for Cu : $AlPO_4$-5: (a) as-synthesised sample; (b) calcined sample.

probably in a tetragonally distorted octahedral environment consistent with its turquoise colour (ref. 2 and references cited therein); it has been shown that the longer axial distances to non-framework oxygen are not always readily revealed in the Fourier transformed EXAFS. This has been attributed to a combination of large Debye–Waller factors and destructive interference with higher shells.[2] However, for the calcined material, the higher multiplicity accords with the copper environment being similar to that in the hexaaquacopper(II) cation as in the Tutton salt[21] and in aqueous solution.[37] Although copper is not substituted into the framework, the EXAFS indicate interactions with the framework through the axial bondings in the calcined sample, consistent with the Cu···Al interaction in the second shell.

Cu : $AlPO_4$-5

The multiplicity (5.0) of the first shell (Cu–O) in the as-synthesised and calcined Cu : $AlPO_4$-5 (Table 1) is probably an average of several copper environments. Attempts to fit the higher shells satisfactorily were unsuccessful, and it would seem that the EXAFS is a convolution of several sites. Although the

Table 1 Results of EXAFS curve-fitting for CuAPO-5/$CuAc_2$ and Cu : $AlPO_4$-5.[a] k-ranges: 3.0–15.0 $Å^{-1}$

Sample		N^b	r/Å	$2\sigma^2/Å^2$	E_0/eV	R (%)
CuAPO-5/$CuAc_2$						
As-synth.	Cu–O	4.0	1.930(2)	0.009(1)	21.0(4)	30.0
	Cu···Cu	1.0	2.931(7)	0.013(1)		
Calcined	Cu–O	6.0	1.929(1)	0.018(3)	21.3(4)	27.6
	Cu···Al[c]	2.0	3.10(2)	0.025(5)		
CuAPO-5/CuO[d]						
As-synth.	Cu–O	4.0	1.992(1)	0.012(1)	21.3(2)	17.9
	Cu···Al	4.0	3.131(4)	0.024(1)		
Calcined	Cu–O	4.0	1.937(3)	0.006(1)	13.6(4)	33.2
	Cu–O	2.0	2.147(8)	0.010(2)		
	Cu···Al	4.0	3.164(8)	0.018(2)		
Cu : $AlPO_4$-5						
As-synth.	Cu–O	5.0	1.941(2)	0.009(1)	21.2(3)	37.0
Calcined	Cu–O	5.0	1.928(2)	0.011(1)	19.3(3)	32.6

[a] Each bonding distance (R, Cu–O) is associated with a coordination number (N) and thermal vibration and static disorder (Debye–Waller-like factor, $2\sigma^2$). E_0 is the refined correction to the threshold energy of the absorption edge. The spectra were Fourier filtered using a Gaussian window function, 1.0–25.0 Å. The standard deviation in the least significant digit as calculated by EXCURV90 is given in parentheses. However, note that such estimates of precision overestimate the accuracy, particularly in cases of high correlation between parameters. The estimated standard deviations for the distances are 0.01 Å at $R<2.5$ Å, with ±20% accuracy for N and $2\sigma^2$, although the accuracy for these is increased by refinements using k^1 *vs.* k^3 weighting (see main text). Residual index R was calculated as

$$R=\frac{\sum_i\left[(\chi_i^{\text{exp}}-\chi_i^{\text{calc}})k^{\text{WT}}\right]^2}{\sum_i\left[(\chi_i^{\text{exp}})k^{\text{WT}}\right]^2}$$

[b] The multiplicities being fixed in the final refinements at the integer closest to the values returned by the full refinements. [c] See main text. [d] Ref. 2.

Table 2 Conversion of propene and nitrogen monoxide for CuAPO-5/$CuAc_2$ and Cu : $AlPO_4$-5

Sample	Temp. max. NO conv./°C	Max. NO conv. (%)	Temp. max. C_3 conv./°C	Max. C_3 conv. (%)
CuAPO-5/$CuAc_2$	400	16.8	500	100.0
Cu : $AlPO_4$-5	500	11.8	500	99.7

XANES shows (Fig. 1) that the as-synthesised and calcined materials have similar electronic surroundings, the Fourier transforms are different showing changes in the local environment upon calcination. The low intensity of the features at 2.5–3.5 Å indicates contributions from the light atoms (non-framework and framework atoms).

deNO$_X$ measurements

Table 2 displays the percentage propene conversions based on CO_2 formation and NO reduction for CuAPO-5/$CuAc_2$ and Cu : $AlPO_4$-5. The only nitrogen containing reduction product observed is N_2. Graphical representations of the NO and propene conversions are shown in Fig. 4 and 5, respectively. There is a difference in the activities of CuAPO-5/$CuAc_2$ and Cu : $AlPO_4$-5. The former exhibits higher propene conversion levels over a wider temperature range and also shows a different trend in NO conversion as compared to Cu : $AlPO_4$-5. In the case of CuAPO-5/$CuAc_2$, NO conversion increases with decreasing temperature from 500 °C to 375 °C followed by a rapid tail-off from this point to lower temperatures. For Cu : $AlPO_4$-5, NO conversion ability falls rapidly from the initial starting temperature of 500 °C, where the NO conversion is 11.8%. Maximium NO conversion is only 16.8% in the case of CuAPO-5/$CuAc_2$ at 400 °C and the maintainance of propene conversion over a wider temperature range is low.

Table 3 shows the standard runs of CuO, empty tube, and CuAPO-5/$CuAc_2$ with no hydrocarbon feed. These results show that there is some slight activity for both propene and NO conversions for CuO compared to the empty tube. Relative to the CuAPO-5/$CuAc_2$ and Cu : $AlPO_4$-5 the activity is minimal. Table 3 also shown that CuAPO-5/$CuAc_2$ does not significantly decompose NO in the absence of the reductant propene.

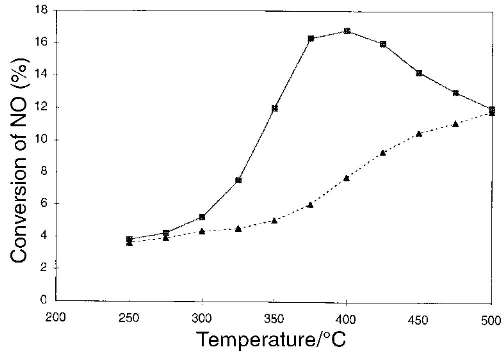

Fig. 4 The NO conversion of CuAPO-5/$CuAc_2$ and Cu : $AlPO_4$-5. ■ CuAPO-5/$CuAc_2$; ▲ Cu : $AlPO_4$-5.

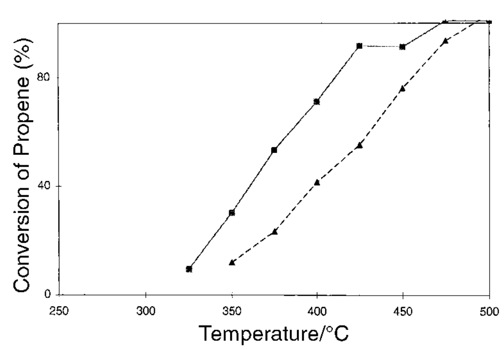

Fig. 5 The propene (C_3) conversion of CuAPO-5/$CuAc_2$ and Cu : $AlPO_4$-5. ■ CuAPO-5/$CuAc_2$; ▲Cu : $AlPO_4$-5.

Table 3 Standard runs of the conversion of propene and nitric oxide of CuO, empty tube and CuAPO-5/$CuAc_2$ with no hydrocarbon feed

	CuO run		Empty tube run		No HC
T/°C	C_3 conv. (%)	NO conv. (%)	C_3 conv. (%)	NO conv. (%)	NO conv. (%)
500	81.1	1.4	35.9	0.2	0.7
475	69.4	2.4	26.2	0.1	1.0
450	48.5	2.4	16.1	0.9	0.8
425	39.5	2.7	12.5	1.2	0.3
400	23.5	2.3	7.3	1.5	0.0
375	14.2	3.3			0.0
350	9.6	2.9			

We have previously shown[2] that CuAPO-5 derived from copper(II) oxide and copper(II) acetate exhibit low activities in the selective catalytic reduction of NO$_X$ in the presence of ammonia and oxygen. This indicates that copper is present in species that are not so amenable to reduction as is the case for the zeolite CuZSM-5 (as seen from XANES (Fig. 1 and ref. 2)) which is necessary for high activity. Of the two, the material derived from copper(II) acetate is more active (53%) than that prepared from copper(II) oxide (27%). Previously reported results have shown that the presence of several copper species and the reduction of copper is necessary for excellent catalytic properties.[16,38] This is consistent with the EXAFS results for CuAPO-5/$CuAc_2$, which show that copper(II) is not sited in the framework. Hence, copper(II) is more available for reduction to copper(I) in the presence of ammonia or hydrocarbons in CuAPO-5/$CuAc_2$ than in the framework substituted CuAPO-5/CuO.

The difference between CuAPO-5 derived from copper(II) acetate and copper(II) oxide may well originate from the different coordination environment. In the calcined CuAPO-5/$CuAc_2$, axial bonding to the framework *via* bridging oxygens was found. In analogy to framework substituted microporous AlPO materials, the lower oxidation state of the copper may well create unsaturation on the connecting aluminium atoms which results in the formation of an acidic OH group. In accordance with the lower activity of the AlPO materials compared to the copper exchanged zeolites (see below), slightly increased activity may originate from the formation of Brønsted acid sites, which interact with the copper ion to form a redox pair.

Cu-ZSM-5 and the CuAPO-5's studied here exhibit very different catalytic activitites in the reduction of NO$_X$, with the former being 100% active.[39] This difference makes a comparison of the two systems interesting. Although the $AlPO_4$'s are zeolite-like they are fundamentally different in that they lack the charged lattice that characterises true zeolites. In accordance with the charged lattice, copper(II) is ion-exchanged into the ZSM-5 structure thereby reducing the number of Brønsted acid sites. Although in principle the $AlPO_4$-5 lattice is neutral, there are reports of weak acidity attributed to lattice imperfections.[18,40] According to Connerton *et al.*[38] it is still not clear whether Brønsted acidity is necessary for the selective catalytic reduction reaction to occur, since it is possible that the Lewis acidity associated with the Cu(I) sites is sufficient to activate the hydrocarbon species.[41]

In any case, it seems likely that the lack of ability to reduce more than a small amount of Cu(II) to Cu(I) for CuAPO-5/$CuAc_2$ is the main reason for the low catalytic activity towards NO$_X$.

Conclusion

(i) Copper(II) acetate unlike copper(II) oxide is not a source for framework substitution of copper. EXAFS shows that the copper environment is tetragonally distorted, and that Cu(O)$_4$ groupings are formed in the as-synthesised sample. In the calcined sample, copper is attached to the framework through [Cu–(O)$_4$–(OAl/P–)$_2$]. (ii) For Cu : AlPO$_4$-5, EXAFS has shown that copper is present in several environments, probably interacting with light atoms as oxygen and framework atoms. (iii) The catalytic measurements show both that CuAPO-5 derived from copper(II) acetate as copper source and that Cu : AlPO$_4$-5 exhibits poor activity in the selective catalytic reduction of NO$_X$ in the presence of hydrocarbons. This is consistent with XANES which has shown that none of the samples undergo autoreduction.

Acknowledgements

Support from the Nansen Foundation and VISTA-Statoil (to D. G. N.) is much appreciated. We thank the Norwegian University of Science and Technology and the Norwegian Research Council for grants towards the construction of the Swiss-Norwegian Beamline (SNBL). The assistance of the SNBL Project Team (W. van Beck, H. Emerich, K. Knudsen, P. Pattison and H. P. Weber) is much appreciated.

References

1 S. T. Wilson, B. M. Lok, C. A. Messina, T. R. Cannan and E. M. Flanigen, *J. Am. Chem. Soc.*, 1982, **104**, 1146.
2 D. G. Nicholson and M. H. Nilsen, *J. Mater. Chem.*, 2000, **10**, 1965.
3 E. M. Flanigen, B. M. Lok, R. L. Patton and S. T. Wilson, *Pure Appl. Chem.*, 1986, **58**, 1351.
4 N. Rajic, D. Stojakovic and V. Kaucic, *Zeolites*, 1991, **11**, 612.
5 C. W. Lee, G. Brouet, X. Chen and L. Kevan, *Zeolites*, 1993, **13**, 565.
6 A. Moen and D. G. Nicholson, *J. Chem. Soc., Faraday Trans.*, 1995, **91**, 3529.
7 T. Muñoz Jr., A. M. Prakash, L. Kevan and K. J. Balkus Jr., *J. Phys. Chem. B*, 1998, **102**, 1379.
8 G. Centi and S. Perathoner, *Appl. Catal. A: General*, 1995, **132**, 179.
9 M. Iwamoto, H. Furukawa, Y. Mine, F. Uemura, S.-I. Mikuriya and S. Kagawa, *J. Chem. Soc., Chem. Commun.*, 1986, 1272.
10 M. Iwamoto and H. Hamada, *Catal. Today*, 1991, **10**, 57.
11 J. Connerton and R. W. Joyner, *Stud. Surf. Sci. Catal.*, 1998, **116**, 327.
12 D.-J. Liu and H. J. Robota, *J. Phys. Chem. B*, 1999, **103**, 2755.
13 P. A. Barrett, G. Sankar, C. R. A. Catlow and J. M. Thomas, *J. Phys. Chem.*, 1996, **100**, 8977.
14 A. Moen, D. G. Nicholson, M. Rønning, G. M. Lamble, J.-F. Lee and H. Emerich, *J. Chem. Soc., Faraday Trans.*, 1997, **93**, 4071.
15 S. Thomson, V. Luca and R. Howe, *Phys. Chem. Chem. Phys.*, 1999, **1**, 615.
16 W. Grünert, N. W. Hayes, R. W. Joyner, E. S. Shpiro, M. R. H. Siddiqui and G. N. Baeva, *J. Phys. Chem.*, 1994, **98**, 832.
17 G. T. Palomino, S. Bordiga, A. Zecchina, G. L. Marra and C. Lamberti, *J. Phys. Chem. B*, 2000, **104**, 8641.
18 N. J. Tapp, N. B. Milestone and D. M. Bibby, in *Innovation in Zeolites Materials Science*, ed. P. J. Grobet, W. J. Mortier, E. F. Vansant and G. Schulz-Ekloff, Elsevier, Amsterdam, 1988, p. 393.
19 *International Tables for X-Ray Crystallography*, The Kynoch Press, Birmingham, UK, 1962.
20 N. Binsted, J. W. Campbell, S. J. Gurman and P. C. Stephenson, EXCALIB, EXBACK and EXCURV90 programs, SERC Daresbury Laboratory, 1990.
21 G. M. Brown and R. Chidambaram, *Acta Crystallogr., Sect. B*, 1969, **25**, 676.
22 H. Jaggi Von and H. R. Oswals, *Acta Crystallogr.*, 1961, **14**, 1041.
23 S. Åsbrink and L.-J. Norrby, *Acta Crystallogr., Sect. B*, 1970, **26**, 8.
24 S. J. Gurman, N. Binsted and I. Ross, *J. Phys. Chem. C*, 1984, **17**, 143.
25 F. W. H. Kampers, C. W. R. Engelen, J. H. C. van Hooff and D. C. Koningsberger, *J. Phys. Chem.*, 1990, **94**, 8574.
26 E. A. Stern, *Phys. Rev. B*, 1993, **48**, 9825.
27 *Report on the International Workshops on Standards and Criteria in XAFS in X-ray Absorption Fine Structure*, ed. S. S. Hasnain, Ellis Horwood, Chichester, 1991, p. 751.
28 R. W. Joyner, K. J. Martin and P. Meehan, *J. Phys. C: Solid State Phys.*, 1987, **20**, 4005.
29 J. M. Bennett, J. P. Cohen, E. M. Flanigen, J. J. Pluth and J. V. Smith, *Intrazeolite Chem., Am. Chem. Soc.*, 1983, 109.
30 W. R. Flavell, D. G. Nicholson, M. H. Nilsen and K. Ståhl, *J. Mater. Chem.*, 2001, **11**, 620.
31 L.-S. Kau, D. J. Spira-Solomon, J. E. Penner-Hahn, K. O. Hodgson and E. I. Solomon, *J. Am. Chem. Soc.*, 1987, **109**, 6433.
32 G. Lamble, A. Moen and D. G. Nicholson, *J. Chem. Soc., Faraday Trans.*, 1994, **90**, 2211.
33 E. Y. Choi, I.-S. Nam, Y. G. Kim, J. S. Chung, J. S. Lee and M. Nomura, *J. Mol. Catal.*, 1991, **69**, 247.
34 S. E. Shadle, J. E. Penner-Hahn, H. J. Schugar, B. Hedman, K. O. Hodgson and E. I. Solomon, *J. Am. Chem. Soc.*, 1993, **115**, 767.
35 I. J. Pickering and G. N. George, *Inorg. Chem.*, 1995, **34**, 3142.
36 J. N. van Niekerk and F. R. L. Schoening, *Acta Crystallogr.*, 1953, **6**, 227.
37 J. D. Lee, *Concise Inorganic Chemistry*, 4th edn., Chapman and Hall, London, 1991, p. 827.
38 J. Connerton, R. W. Joyner and M. Stockenhuber, *Chem. Commun.*, 1997, 185.
39 M. Iwamoto, H. Yahiro, K. Tanda, N. Mizuno, Y. Mine and S. Kagawa, *J. Phys. Chem.*, 1991, **95**, 3727.
40 C. Halik, A. Lercher and H. Mayer, *J. Chem. Soc., Faraday Trans. 1*, 1988, **84**, 4457 and references therein.
41 J. Connerton, M. B. Padley and R. W. Joyner, *J. Chem. Soc., Faraday Trans.*, 1995, **91**, 1841.